02.56.20 g'

Determination of Neutron Spectra with Nuclear Plates and Its Application to the Measurement of the Be^8 Excitation Levels

By Emma Perez Ferreira and Pedro J. Waloschek,* Argentina

I. EXPERIMENTAL TECHNIQUE

Introduction

Powell[1] called attention to the possibility of using nuclear plates for the determination of fast neutron spectra. Gibson and Livesey[2] subsequently developed a method for such determinations, which was followed by most of the later workers. Richards[3] also suggested a similar method which, while it was easier for experimental purposes, has the disadvantage of a low spectral resolution. A method used at the Los Angeles laboratory (California), and described in detail by Allred and Armstrong,[4] shows a similar disadvantage. Rosen[5] compiled over 60 references to publications on the subject.

Generally speaking, those methods entail the measurement of the angle of emergence θ and of the energy E_p of the recoil protons produced by impacts with the H nuclei of the emulsion of a plate so placed as to be grazed by the neutron beam (Fig. 1). These data serve as the starting point for computing the number of incident neutrons N and their energy E_n by means of equations:

$$dP = N(E) \cdot \sigma(E) \cdot A \cdot V \cdot \frac{\cos\theta}{\pi} \cdot d\Omega \cdot \Delta E \qquad (1)$$

$$E_p = E_n \cos^2\theta \qquad (2)$$

in which dP is the number of protons emitted by the neutrons in the energy interval ΔE, into the element of solid angle $d\Omega$. V is the volume and A the H content of the emulsion. $\sigma(E)$ is the neutron-proton scattering cross section.

Gibson and Livesey compute E_n by means of Equation 2, using, for each proton, its angle θ with the direction of incidence of the neutron beam; on the other hand, Richards, Allred and Armstrong measure only those tracks whose θ angle is so small that it may be assumed that the proton carries practically all the energy of the neutron which produced it, i.e., $E_n = E_p$, except for a correction factor obtained by averaging $\cos^2\theta$ over the whole of the solid angle containing the tracks. While this last method affords a great saving of time and work, since all the angular measurements are eliminated and the computations are simplified, its low resolving power makes the Gibson and Livesey method preferable.

Any high resolution method implies the computation of the energy of several thousands of protons, based on the microscopic measurement of one length and two angles for each of them. This means that in the measurement work it is important to apply criteria of selection which are sufficiently strict so as to avoid waste of time on proton tracks that would later be discarded for not being in the energy range in which it is intended to work, and also to simplify the computation of the energies and corrections using nomograms and tables in case electronic machines are unavailable.

This work was undertaken with that purpose in mind. Essentially the Gibson and Livesey method is followed, but the selection criteria are basically modified in order to obtain the greatest possible efficiency in the energy range for which information is sought, and to make a simple function available for the computation of the corrections for the efficiency of the method and for the emergence of tracks from the emulsion.

Selection of Tracks

The proton tracks to be measured are selected so that their projection along the direction of neutron incidence (x) is greater than a constant R_0, and that the angle with that same direction θ, is less than 45 degrees. This last criterion is applied, in part, during microscopic examination, and is completed after the computations have been made. Thus a fraction of the protons is selected, the energy of which is greater than $E_0 = (R_0/a)^{1/b}$, where a and b are constants of the emulsion.

Measurement

Measurements for each proton selected (Fig. 2) include: the angle α formed by the projection of the track on the plane of the plate with the direction x; the angle φ formed by the track and the plane of the plate; and the length L, of the projection of the track on the plane of the plate.

In order that the deviation of the track from its original direction, produced by scattering, distortion,

Original language: Spanish.

* Comisión Nacional de la Energía Atómica, Argentina.

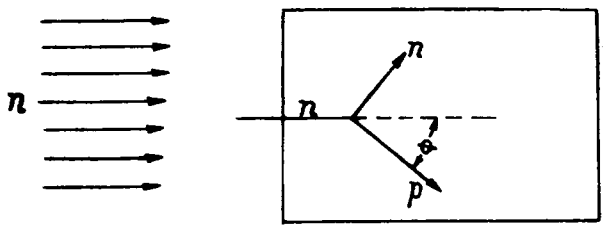

Figure 1

etc., should not affect the measurement, the angle α will be taken to be the one formed by the direction x and the tangent at the origin of the direction of the track. The angle φ is measured by taking the difference in depth (Δz) between the origin of the track and a point 100 divisions away from it on the optical scale.

The determination and recording of the data are carried out at a rate of about 10 protons per hour per person, using a binocular microscope (Ortholux) with a 100× immersion objective lens and a 10× eyepiece. (With this combination, the scale calibration gave: 100 divisions = 111 microns.) L is measured on the optical scale, following the track.

Computation of the Energy

The energy E_n of the neutron responsible for each recoil is derived from these data by applying formulae:

$$E_p = E_n \cos^2 \theta \qquad (2)$$

$$R = a \cdot E_p^b \qquad (3)$$

$$\cos \theta = \cos \alpha \cdot \cos \varphi \qquad (4)$$

where R is the range of the proton and E_p its energy.

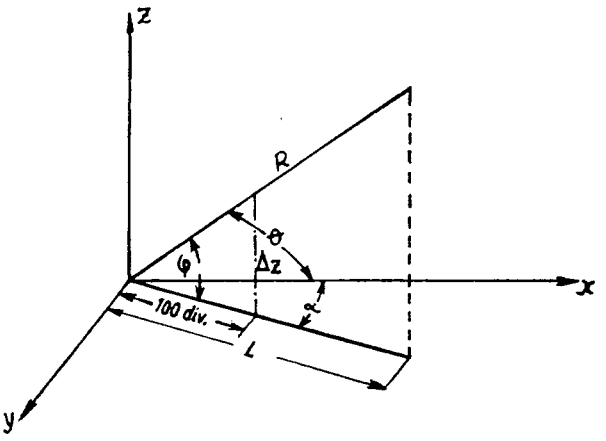

Figure 2

From Equations 2, 3 and 4, one can write:

$$a \cdot E_n^b = R(E) = \frac{L}{\cos^{2b+1} \varphi \cdot \cos^{2b} \alpha} \qquad (5)$$

The terms $\cos^{2b+1} \varphi$ and $\cos^{2b} \alpha$ are derived from Δz and α (in degrees) by means of a nomogram which also gives the value of θ (Fig. 3). This nomogram should be constructed especially for each plate, since the individual shrinkage factor modifies the scale on which Δz actually is measured.

For subsequent use of the data, and for checking purposes, a tabulation of the values for $\cos^{2b+1} \varphi$, $\cos^{2b} \alpha$ and θ is convenient.

The values for E are taken from a chart, or even better, from the 0.1 Mev tables of the US AEC (1953) corresponding to the Lattes *et al.* data of 1947.[6]

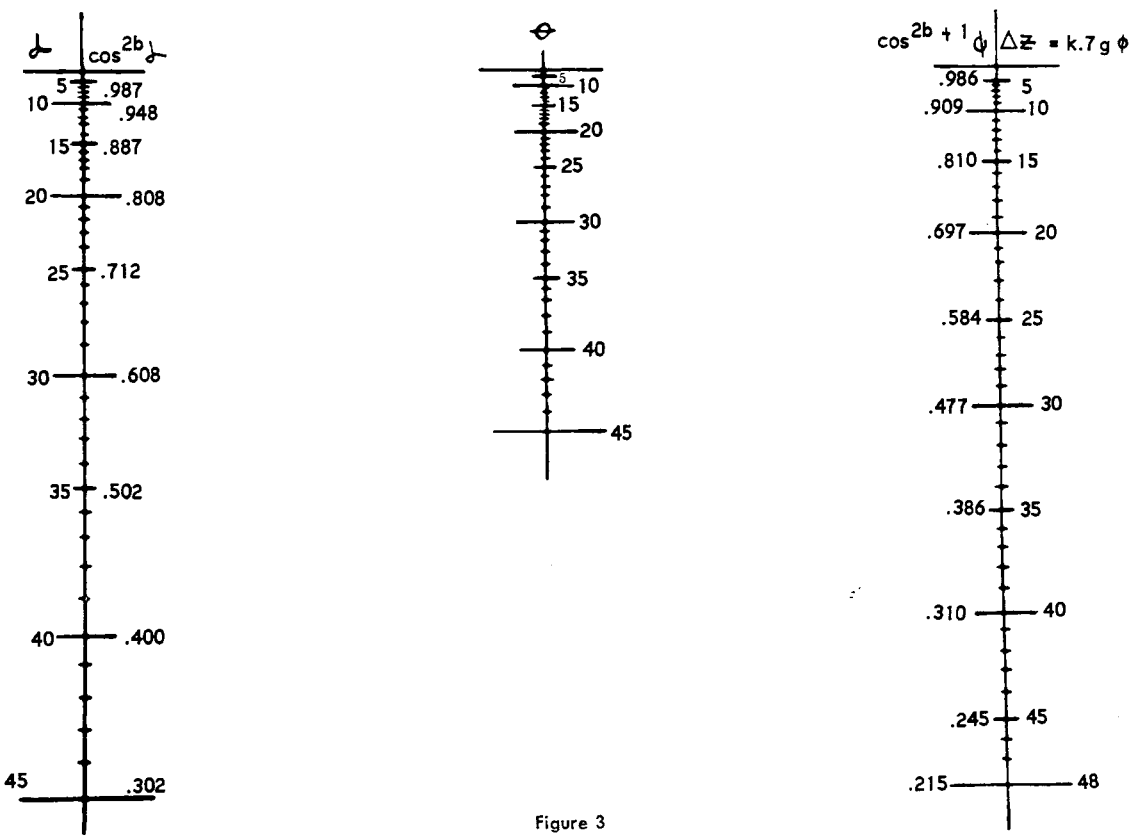

Figure 3

Evaluation of the Spectrum

Construct, with the E values obtained, an histogram $P(E_n)$, in which the interval ΔE is to be taken as small as possible, which, in this case, according to the resolution of the method, could be 0.1 Mev. In passing from the histogram to the curve $P(E_n)$ it is convenient, in order to avoid dispersion of the data, to increase the interval, for instance to $3\Delta E$.

In order to compensate for the consequent decrease in the number of points used for charting, it is convenient, instead of using the successive increased intervals, to have them partially overlap, in such a way as again to have data for each ΔE. The curve will be drawn through the points obtained by averaging the three possible ordinates which, in this case, will belong to each ΔE interval; this is the equivalent of a weighted average between the values for the interval in question and those adjacent to it.

In effect, the graphical method used yields:

$$P(\Delta E_i) = \frac{P(\Delta_3 E_{i+1}) + P(\Delta_3 E_i) + P(\Delta_3 E_{i-1})}{3} = \frac{3P(\Delta E_i) + 2[P(\Delta E_{i+1}) + P(\Delta E_{i-1})] + [P(\Delta E_{i+2}) + P(\Delta E_{i-2})]}{3}$$

where $P(\Delta_3 E_i)$ is the ordinate corresponding to the increased interval which includes the simple intervals ΔE_{i-1}, ΔE_i and ΔE_{i+1}.

The resulting curve coincides, within less than 10^{-3}, with the one obtained by the usual method of polynomial approximation, in this case, of the second degree.

The errors of curve $P(E)$ also are easily obtained by joining the maximal and minimal values of consecutive intervals, as may be seen on Fig. 4.

The obtained $P(E)$ values are tabulated with 0.1 Mev intervals in order that the relevant corrections might be applied in passing from the proton to the neutron spectrum $N(E)$.

Corrections

The $P(E)$ curve, above, represents the neutron spectrum $N(E)$, multiplied by the (n,p) scattering cross section $\sigma(E)$, and a factor due to track suppression according to the selection criteria used, $A(E)$, and to emulsion emergence, $B(E)$ and $C(E)$:

$$P_1(E) = V \cdot A \cdot N(E) \cdot \sigma(E) \cdot \Delta E[1 - A(E) - B(E)] \quad (6)$$

where E is such that

$$R_0 \leq R(E) \leq \frac{R_0}{\cos^{2b+1} 45 \text{ degrees}}$$

and

$$P(E) = \tfrac{1}{2}A \cdot V \cdot N(E) \cdot \sigma(E) \cdot \Delta E[1 - C(E)] \quad (7)$$

where E is such that:

$$R(E) > \frac{R_0}{\cos^{2b+1} 45 \text{ degrees}}$$

in which V is the revised volume of the emulsion, A the number of H atoms per cm^3 of emulsion, and

$$A(E) = \left[\frac{R_0}{R(E)}\right]^{2/2b+1} = \cos^2\theta(E) \quad (8)$$

$$B(E) = \frac{4R(E)}{\pi h}\int_0^{\theta(E)} \cos^{2b+1}\theta \sin^2\theta\, d\theta = \frac{4R_0}{\pi h}\left[\frac{R(E)}{R_0}\int_0^{\theta(E)} \cos^{2b+1}\theta \sin^2\theta\, d\theta\right] = \frac{4R_0}{\pi h} B'E \quad (9)$$

$$C(E) = \frac{0.1656}{h} \cdot R(E) \quad (10)$$

All these corrections are applicable provided that (See Appendix):

$$h > 0.303R(E)$$

The integral given in Equation 9 was computed numerically and plotted with enough accuracy to obtain its values as a function of $R_0/R(E)$ through

$$\cos^{2b+1}\theta(E) = \frac{R_0}{R(E)} \quad (11)$$

shown in the same graph (Fig. 5). The data obtained appear on Table I, together with the values for:

$$1 - A(E) = \sin^2\theta(E) \quad (12)$$

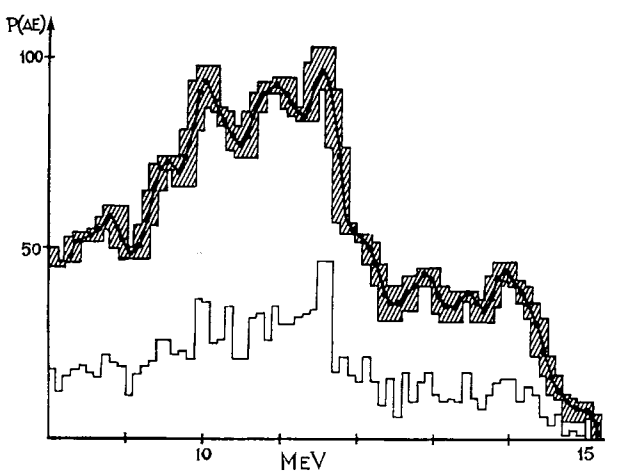

Figure 4

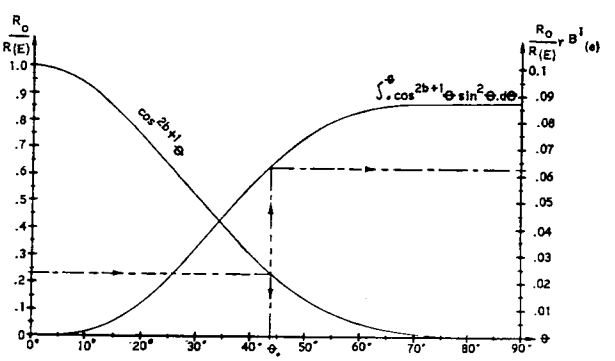

Figure 5

The total correction for selection and escape, for each energy interval in which Equation 6 holds good, is obtained, for a given R_0 and h, by computing first the corresponding $R_0/R(E)$, and then applying the values of Table I to Equation 6. We obtained the values appearing in Fig. 6 for $R = 111$ microns and $h = 400$ microns. A tabulation in function of $R_0/R(E)$ when Equation 7 should be applied was not deemed necessary, due to the simplicity of the relationship it expresses. Figure 6 also includes the resulting values of the aforementioned R_0 and h in this energy interval.

II. DETERMINATION OF THE NEUTRON SPECTRUM FOR THE Li(d,n)Be REACTION

Li(d,n)Be Reaction Neutrons

The bombardment of lithium with deuterium in the accelerator is one of the methods most used for obtaining neutrons over a spectrum extending up to 15 Mev. Richards[3] determined the energy of these neutrons in 1941, and Green and Gibson[4] improved the measurement in 1949; the spectrum produced by Li^6 and by Li^7 also was observed. Trumpy *et al.*[9] measured, in

Table I

$R_0/R(E)$	θ_0'	B'	$1-A$	$R_0/R(E)$	θ_0'	B'	$1-A$
0.00	90 00	∞	1.000	0.50	31 10	0.068	0.268
0.01	70 00	8.65	0.883	0.51	30 40	0.065	0.260
0.02	65 50	4.28	0.832	0.52	30 20	0.062	0.255
0.03	63 20	2.83	0.799	0.53	29 50	0.059	0.248
0.04	60 50	2.09	0.763	0.54	29 25	0.056	0.241
0.05	59 10	1.66	0.737	0.55	29 00	0.053	0.235
0.06	57 50	1.36	0.717	0.56	28 35	0.051	0.229
0.07	56 40	1.15	0.698	0.57	28 10	0.048	0.223
0.08	55 30	0.996	0.679	0.58	27 45	0.046	0.217
0.09	54 20	0.873	0.669	0.59	27 20	0.043	0.211
0.10	53 20	0.775	0.643	0.60	26 55	0.041	0.205
0.11	52 30	0.695	0.629	0.61	26 30	0.039	0.199
0.12	51 40	0.628	0.615	0.62	26 10	0.037	0.193
0.13	50 50	0.571	0.601	0.63	25 40	0.035	0.188
0.14	50 00	0.522	0.587	0.64	25 10	0.033	0.181
0.15	49 05	0.480	0.571	0.65	24 45	0.031	0.175
0.16	48 25	0.443	0.560	0.66	24 20	0.029	0.170
0.17	47 45	0.411	0.548	0.67	23 55	0.027	0.164
0.18	47 05	0.382	0.536	0.68	23 25	0.026	0.158
0.19	46 30	0.356	0.526	0.69	23 00	0.024	0.153
0.20	45 55	0.333	0.516	0.70	22 35	0.023	0.148
0.21	45 15	0.311	0.504	0.71	22 15	0.021	0.143
0.22	44 40	0.292	0.494	0.72	21 45	0.020	0.137
0.23	44 05	0.275	0.484	0.73	21 20	0.019	0.132
0.24	43 30	0.259	0.474	0.74	20 55	0.018	0.128
0.25	42 55	0.244	0.464	0.75	20 25	0.016	0.122
0.26	42 20	0.230	0.454	0.76	19 55	0.015	0.116
0.27	41 50	0.217	0.445	0.77	19 25	0.014	0.111
0.28	41 20	0.206	0.436	0.78	18 55	0.013	0.105
0.29	40 45	0.195	0.426	0.79	18 25	0.012	0.100
0.30	40 15	0.185	0.418	0.80	18 00	0.011	0.096
0.31	39 50	0.175	0.410	0.81	17 25	0.010	0.090
0.32	39 15	0.166	0.400	0.82	16 55	0.010	0.085
0.33	38 45	0.158	0.392	0.83	16 25	0.009	0.080
0.34	38 15	0.150	0.383	0.84	15 50	0.008	0.074
0.35	37 50	0.143	0.376	0.85	15 25	0.007	0.071
0.36	37 20	0.136	0.368	0.86	14 45	0.007	0.065
0.37	36 50	0.129	0.359	0.87	14 15	0.006	0.061
0.38	36 25	0.123	0.352	0.88	13 30	0.005	0.055
0.39	36 00	0.117	0.346	0.89	13 00	0.005	0.051
0.40	35 30	0.111	0.337	0.90	12 30	0.004	0.047
0.41	35 05	0.106	0.330	0.91	11 50	0.003	0.042
0.42	34 40	0.101	0.324	0.92	11 05	0.003	0.037
0.43	34 10	0.096	0.315	0.93	10 30	0.002	0.033
0.44	33 45	0.092	0.309	0.94	9 40	0.002	0.028
0.45	33 15	0.087	0.301	0.95	8 50	0.001	0.024
0.46	32 50	0.083	0.294	0.96	8 00	0.001	0.019
0.47	32 25	0.079	0.287	0.97	7 00	0.001	0.014
0.48	32 00	0.075	0.281	0.98	6 00	0.000	0.011
0.49	31 35	0.072	0.273	0.99	4 10	0.000	0.005

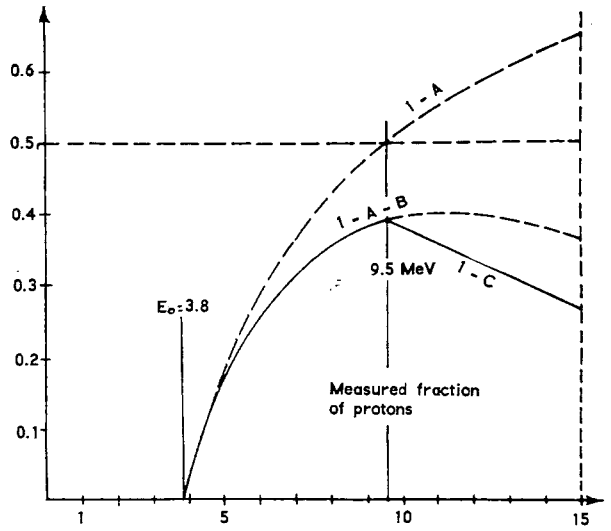

Figure 6

1952, the spectrum obtained with seven different angles relative to the direction of the deuterons, thus also obtaining the angular distribution. The energy values obtained for the peaks of the spectrum by the different authors (excepting Richards, whose resolution was poor) are in substantial agreement and give good information on the Be^8 and Be^7 excitation levels. However, the intensity of the peaks found shows differences due to several factors, particularly to the dependence on the geometry of the Li target and the criteria on selection of tracks used.

Exposure and Development of the Plates

Plates were exposed about the Li target of the C.N.E.A. cascade accelerator (Buenos Aires), in the positions shown in Fig. 7, between -150 and $+150$ degrees, for 12.9 μa-hr and at 900 kv. The distance from the source was 22 cm.

Ilford G5, 2×3 in., 400 micron plates were used; development was carried by the Dainton *et al.*[10] (1951; Bristol) hot-plate method. About nine days of processing are required before a plate ready for microscopy is obtained.

Notwithstanding the G5 plate sensitivity to electrons, the background produced by the exposure was not excessive, and, on the other hand, one had the advantage of good proton track visibility ("black" tracks). Previous trial exposures at 0 and 90 degrees had been made, from which the plates used for another determination of the spectrum of the same reaction were obtained, using a graphical method (1953).[11]

Leitz 24:1, 53:1 and 100:1 special nuclear plate objective lens sets were used for the measurements, particularly the latter, and $10 \times$ eyepiece pairs, one with a scale, and the other with a grid.

Spectra at 0 and 90 Degrees

Among the plates exposed as above, those at 0 and at 90 degrees were selected while, at 0 ± 1 and 90 ± 1 degrees, respectively, the recoil protons were selected according to the criterion explained earlier, and in volumes 5 to 10 mm from the edge of the plate closer to the Li target.

Figures 8 and 9 show the results obtained in the determination of the neutron spectrum, including the emergence, efficiency and cross-section corrections.

In both cases, the applicability condition of the method ($h > 0.303\ R(E)$) applied, since the range of the protons of maximal energy obtained in the reaction under study (15 Mev), was about 1140 microns, and 400 micron plates were used.

III. CONCLUSIONS

Be^8 Excitation Levels

As already shown by Green and Gibson (1949)[7] the neutrons of over 5 Mev produced in lithium by the deuterium can only come from reactions:

$$Li^7 + d \rightarrow Be^8 + n$$

$$Li^7 + d \rightarrow \alpha + \alpha + n$$

The former produces neutrons in individual groups, since the Be^8 may remain excited, a condition which is in agreement with observations made in the course of other experiments, while the latter produces neutrons having energies showing the characteristic spectral distribution of disintegration into three particles.

The Q of the first reaction above may be computed for the neutron spectrum peaks, allowing for the neutron emission angle and the incident deuterium energy (where the loss of energy of the deuterium in the thick lithium target should be observed). Q was computed in this fashion for the measured spectra, to which were added those of the papers published by Green and Gibson,[7] and Trumpy *et al.*,[9] and all were

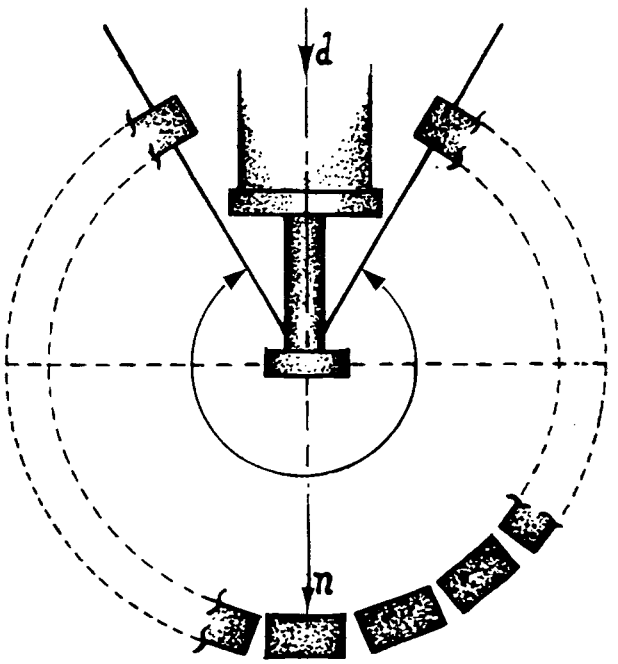

Figure 7

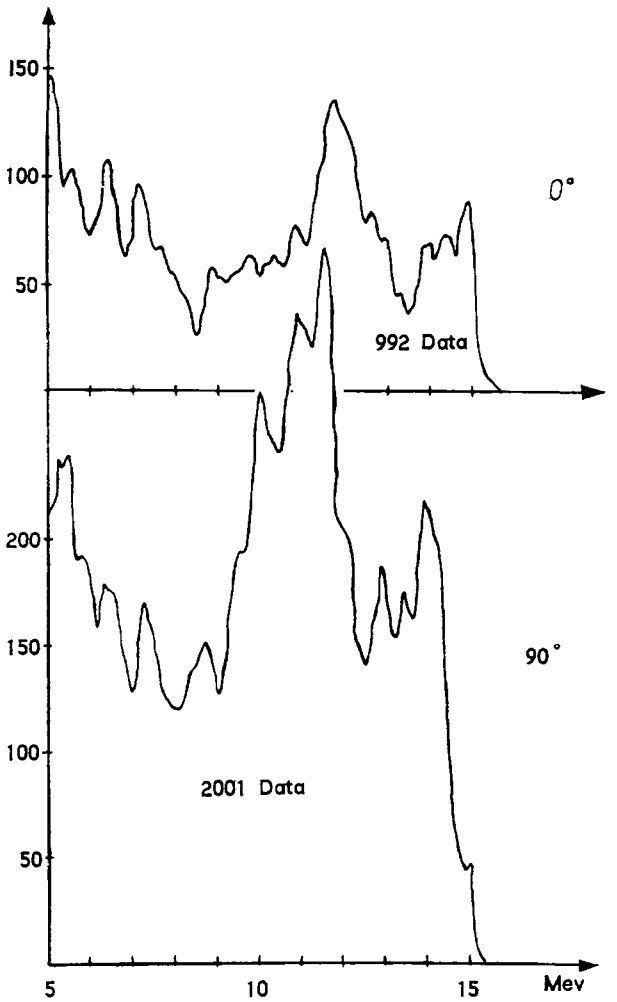

Figure 8. (Above) Figure 9. (Below)

grouped in Fig. 10. To the spectra given by these authors (solid line), we added a dotted line connecting the experimental data.

Perfect coincidence of the 15 Mev peak is observed in all the measurements.

The other observed peaks were those corresponding to 2.8, 3.4, 4.2 and 5.0 Mev Be^8 excitation energies, of which the 2.8 and 3.4 levels have not been resolved to date, although they are suggested by all the data gathered so far.

These peaks are verified by other reactions in which the Be^8 excitation levels come into play (see Green and Gibson[7]). This is not true of the other peaks that may be observed but, when computing the value of Q they do not coincide. These are probably due to impurities in the target or to mutual actions with the target holder.

Note:

The Richards (R) data of over 6 Mev are statistically poor, since they were measured from 2 Mev, and the greater part of the neutrons (4/5) are accumulated between 2 and 5.

The Trumpy *et al.* data (B) were taken from a short abstract published in *Nature* (1952). The complete data published in Bergen (1953), were not received at Buenos Aires.

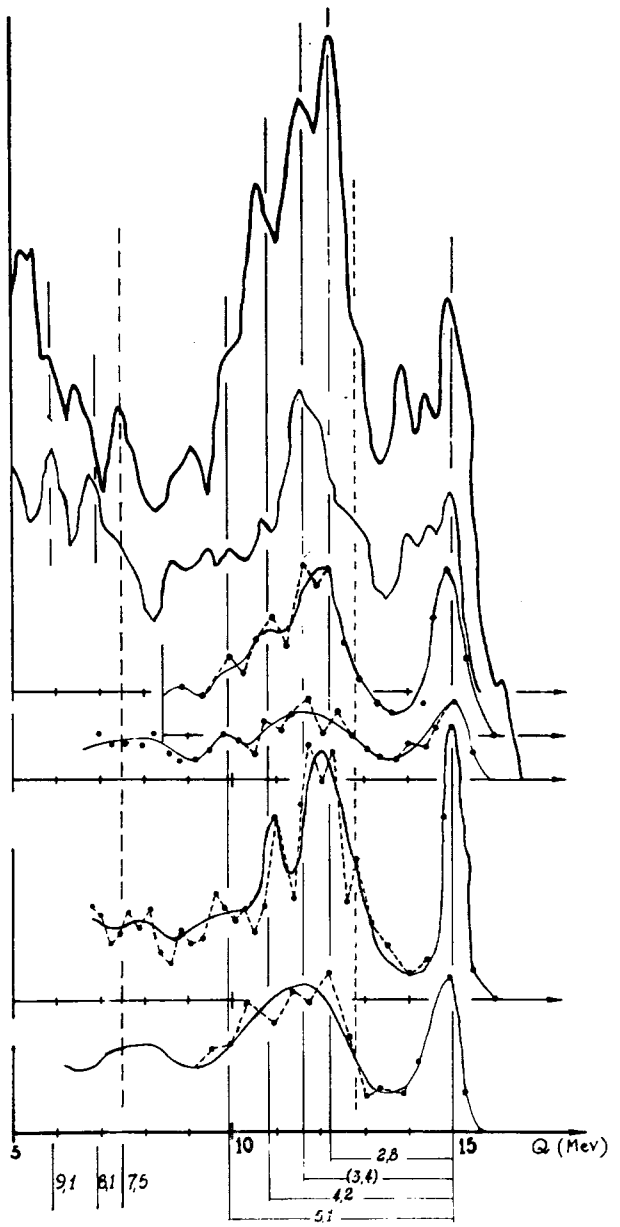

Figure 10

The Green and Gibson (G & G) data above 7.5 Mev are not corrected for emergence, so that the relevant ordinates are not comparable with other measurements. The small thickness of the plates used in most of the work (100 microns) greatly reduces the number of the protons between 11 and 15 Mev.

Method Used

It has been possible, by the selection criteria used in the high resolution method (chapter II) to map out the area of the spectrum in which measurements are taken (See efficiency curve, Fig. 6). This eliminates the superfluous data and greatly improves the statistics in the maximal efficiency zone which, on the other hand, may be selected according to the spectrum being studied, taking the appropriate R_0 and θ_{lim} parameters.

In this fashion the greater part of the measured data were obtained in the 8 to 13 Mev zone, giving great precision in the details of the peaks grouped about 11 Mev in the 90 degree spectrum. In these peaks, the data obtained within each 0.3 Mev interval are of the order of 50 in each 1000 measured protons while Richards, for example, gets some 5 per 1000 protons measured, over a 0.4 Mev interval.

With only two microscope operators some 1000 data are collected in about a fortnight by the high resolution method, which if they fall within a zone of the spectrum which is not unduly wide, do give good information on it.

APPENDIX

Computation of Corrections

From Equations 2 and 3 one can find out that the range of a proton produced by a neutron of energy E_n, which forms an angle θ with the direction of the incidence of the latter is:

$$R_p = a \cdot E_n^b \cdot \cos^{2b} \theta \qquad (13)$$

where $a \cdot E_n^b$ represents the range of a proton having the energy E_n of the incident neutron, which we shall express as:

$$a \cdot E_n^b = R(E)$$

Thus:

$$R_p = R(E) \cos^{2b} \theta \qquad (14)$$

It will be seen here that all the recoil proton tracks created in the same elementary volume by monoenergetic neutrons will end over surfaces defined by the $R = K(\cos^{2b}\theta)$ equation. Once they are drawn for the different energies, the cross sections of these surfaces will show the outline indicated in Fig. 11 (assuming that $b = 1.725$), serving as the base for the development of the graphical method for the determination of the neutron spectra mentioned in Section II.

On the other hand, the number of recoil protons originated in a $s \cdot dz$ volume of emulsion located at depth z, with A atoms of H per cm^3, crossed by $N(E)$ neutrons of an energy included in the interval ΔE, and which are emitted within solid angle $d\Omega$, forming angle θ with the direction of neutron incidence is:

$$dP = A \cdot s \cdot N(E) \cdot \sigma(E,\theta) \cdot d\Omega \cdot dz\, \Delta E \qquad (15)$$

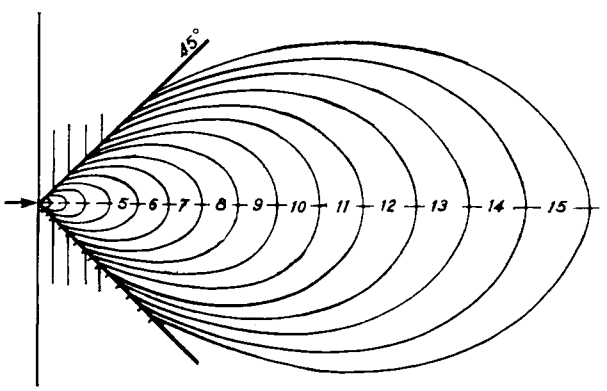

Figure 11

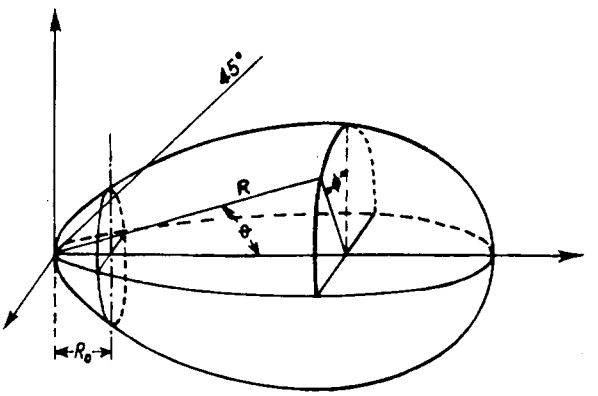

Figure 12

with $\sigma(E,\theta) = (\sigma(E) \cos \theta)/\pi$ the (n,p) differential cross section and $(d\Omega)$ the solid angle which, in our case, is $d\Omega = \sin \theta\, d\theta\, d\phi$ (Fig. 12), from which the total number of protons produced by the neutrons in interval ΔE will be:

$$P(E) = \frac{A}{\pi} \cdot s \cdot N(E) \cdot \sigma(E) \int_z \int_\theta \int_\phi \sin \theta \cos \theta\, d\theta\, d\phi\, dz\, \Delta E \qquad (16)$$

The limits for each one of the successive integrations will be deduced from the conditions resulting from the selection of the tracks for their measurements: (*a*) angle formed with the direction of incidence smaller than 45 degrees: $\theta < 45$ degrees; (*b*) projection of the track on direction x, greater than a constant value: $R(E) \cos^{2b+1} \theta > R_0$; and (*c*) trace totally contained in the emulsion: $R(E) \cos^{2b} \theta \sin \theta \cos \phi < z$.

In order to be able to judge the physical meaning of the integration limits thus derived, the following reasoning may be used (Fig. 13).

For a given energy, and for each θ direction, there is a boundary or limiting value z_0 such that, for each value $z < z_0$ a part of the relevant protons escape from the emulsion through its surface ($z = 0$); while on the other hand, for $z > z_0$, all the recoil protons produced with such an angle will have been counted since their tracks end within the emulsion.

Therefore, within the first zone, i.e., for $0 < z < z_0$, there will remain, within the emulsion, those protons

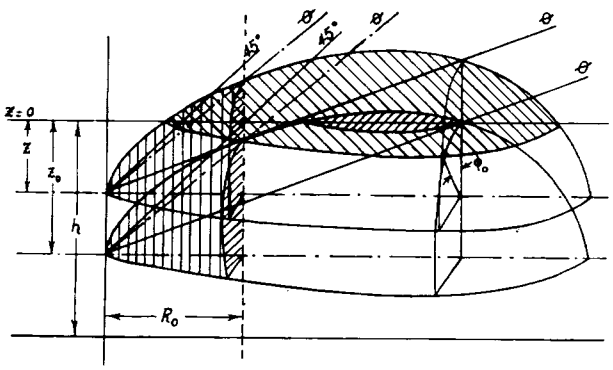

Figure 13

whose ϕ would be larger than a ϕ_0, minimum ϕ_0, which is the one deduced from condition (*c*)

$$\phi_0 = \arccos \frac{Z}{R(E) \cdot \cos^{2b} \theta \cdot \sin \theta} \tag{17}$$

and, if we consider only the upper "half lobes" (related to the emergence through the surface of the emulsion), all those protons whose ϕ is such that $\pi/2 > \phi > \phi_0$ will have been counted.

On the other hand, for $z_0 < z < h$ (h is emulsion thickness) it was observed that all the protons would be counted regardless of their ϕ. The value z_0 is also deduced from conditions (*c*) for

$$\phi = 0, \qquad (\cos \phi = 1)$$

or, it is:

$$Z_0 = R(E) \cdot \cos^{2b} \theta \sin \theta \tag{18}$$

Therefore the integration of Equation 16 should be carried out leaving the integral over ϕ for last, as follows:

$$P(E) = \frac{2A}{\pi} sN(E)\sigma(E) \int_\theta \left[\int_{z=0}^{z_0} 2 \int_{\phi=\phi_0}^{\pi/2} \sin \theta \cos \theta \, d\phi \, dz + \int_{z_0}^{h} 2 \int_0^{\pi/2} \sin \theta \cos \theta \, d\phi \, dz \right] d\theta \, \Delta E \tag{19}$$

in which the factors 2, in the two terms within the bracket, complete the rear part of each half lobe, and the 2 applied to the expressions as a whole causes the contribution of the lower half lobes and resulting emergence through the lower surface of the emulsion to be taken into account.

Regarding the integral over θ, it will suffice to take it between 0 and a θ_0 deduced from condition (*b*)

$$\theta_0 = \arccos \left[\frac{R_0}{R(E)} \right]^{\frac{1}{2b+1}} \tag{20}$$

provided this θ_0 is smaller than 45 degrees (case shown on Fig. 13). If not, it will be taken only between 0 and 45 degrees (case shown on Fig. 13). Therefore, it will be necessary to split Equation 19 in two parts, obtaining:

for $$R_0 < R(E) < \frac{R_0}{\cos^{2b+1} 45 \text{ degrees}}:$$

$$P_1(E) = 2 \frac{A}{\pi} sN(E)\sigma(E) \int_{\theta=0}^{\theta_0} \left[\int_{z=0}^{z_0} 2 \int_{\phi=\phi_0}^{\pi/2} \sin \theta \cos \theta \, d\phi \, dz + \int_{z_0}^{h} 2 \int_0^{\pi/2} \sin \theta \cos \theta \, d\phi \, dz \right] d\theta \, \Delta E \tag{21}$$

and for:

$$R(E) > \frac{R_0}{\cos^{2b+1} 45 \text{ degrees}}:$$

$$P_2(E) = 2 \frac{A}{\pi} sN(E)\sigma(E) \int_{\theta=0}^{\pi/2} \left[\int_{z=0}^{z_0} 2 \int_{\phi=\phi_0}^{\pi/2} \sin \theta \cos \theta \, d\phi \, dz + \int_{z_0}^{h} 2 \int_0^{\pi/2} \sin \theta \cos \theta \, d\phi \, dz \right] d\theta \, \Delta E \tag{22}$$

After computing both integrals, we have, taking $V = s\,h$:

$$P_1(E) = AVN(E)\sigma(E) \left[1 - \left(\frac{R_0}{R(E)} \right)^{2/2b+1} - \frac{4R(E)}{\pi h} \int_0^{\theta_0} \cos^{2b+1} \theta \sin^2 \theta \, d\theta \right] \Delta E \tag{23}$$

$$P_2(E) = \frac{A}{2} VN(E)\sigma(E) \left[1 - \frac{0.1656}{h} R(E) \right] \Delta E \tag{24}$$

in which one can see the correction terms due to intersection with a plane at distance R_0 and to the emergence of tracks from the emulsion in the first expression and only this last condition in the second.

An indispensable requirement yet has to be taken into consideration in order that this result be valid. When referring to the integration over z we said that there was no emergence from the emulsion for $z_0 < z < h$; this means that it is a necessary condition for this reasoning that $h > z_0$ and, since this should happen for all possible directions of θ, it is a necessary condition that $h > \max [z_0]$, a value easily obtained by making the z_0 differential equal to zero:

$$-2b \cdot R(E) \cos^{2b-1} \theta \sin^2 \theta + R(E) \cos^{2b+1} \theta = 0$$

Solving:

$$\cos^2 \theta - 2b \sin^2 \theta = 0 \qquad \tan \theta = \sqrt{\frac{1}{2b}}$$

Therefore:

$$\max [z_0] = R(E) \cdot \frac{(\frac{1}{2}b)^{\frac{1}{2}}}{(1 + \frac{1}{2}b)^{b+\frac{1}{2}}}$$

and:

$$\max [z_0] = 0.303 \cdot R(E) \tag{25}$$

REFERENCES

1. Powell, *Further applications of the photographic method in nuclear physics*, Nature, 145, 155, Bristol (1940).
2. Gibson and Livesey, *The neutrons emitted in the disintegration of nitrogen by deuterons*, Proc. Phys. Soc., 60, 523, Cambridge (1948).
3. Richards, *A photographic plate spectrum of the neutrons from the disintegration of lithium by deuterons*, Phys. Rev., 59, 796, Texas (1941).
4. Allred and Armstrong, *Laboratory handbook of nuclear microscopy*, Report of Los Alamos Scientific Laboratory, USAEC (1953).
5. Rosen, *Nuclear emulsion techniques for the measurement of neutron energy spectra*, Nucleonics, July and August (1953).
6. Lattes, Fowler and Cuer, *A study of the nuclear transmutations of light elements by the photographic method*, Proc. Phys. Soc. 59, 883, Bristol (1947).
7. Green and Gibson, *The neutrons emitted in the disintegration of lithium by deuterons*, Proc. Phys. Soc., 62, 407, Cambridge (1949).
8. Green and Gibson, *The neutrons emitted in the bombardment of Li^6 by deuterons*. Proc. Phys. Soc., 63, 494, Cambridge (1950).
9. Trumpy, Grodtal and Graue, *Angular distribution of the neutrons from the reaction Li^7 (d,n) Be^8*, Nature, 170, 1118, Bergen (1952).
10. Dainton, Gattiker and Lock, *The processing of thick photographic emulsions*, Phil. Mag., Ser. 7, 42, 396, Bristol (1951).
11. Waloschek, Pérez Ferreira and Roederer, *Un método gráfico para la determinación de espectros de neutrones rápidos*, Communicación a la Asociación Física Argentina, Buenos Aires (1953).